Int. J. Exp. Path. (2008), 89, 350–357
doi: 10.1111/j.1365-2613.2008.00600.x

ORIGINAL ARTICLE

Temporal evolution of epithelial, vascular and interstitial lung injury in an experimental model of idiopathic pulmonary fibrosis induced by butyl-hydroxytoluene

Edwin Roger Parra, Gabriela Boufelli, Fernanda Bertanha, Luciana de Paula Samorano, Armando Costa Aguiar Junior, Fernanda Magalhães Arantes Costa, Vera Luiza Capelozzi and João Valente Barbas-Filho

Departamento de Patologia, Faculdade de Medicina da Universidade de São Paulo, São Paulo, SP, Brazil

INTERNATIONAL JOURNAL OF EXPERIMENTAL PATHOLOGY

Summary

This study was undertaken to test whether the structural remodelling of pulmonary parenchyma can be sequentially altered in a model and method that demonstrate the progression of the disease and result in remodelling within the lungs that is typical of idiopathic pulmonary fibrosis. Three groups of mice were studied: (i) animals that received 3-5-di-*tert*-butyl-4-hydroxytoluene (BHT) and were killed after 2 weeks (early BHT = 9); (ii) animals that received BHT and were killed after 4 weeks (late BHT = 11); (iii) animals that received corn oil solution (control = 10). The mice were placed in a ventilated Plexiglas chamber with a mixture of pure humidified oxygen and compressed air. Lung histological sections underwent haematoxylin–eosin, immunohistochemistry (epithelial, endothelial and immune cells) and specific staining (collagen/elastic fibres) methods for morphometric analysis. When compared with the control group, early BHT and late BHT groups showed significant decrease of type II pneumocytes, lower vascular density in both and higher endothelial activity. CD4 was increased in late BHT compared with early and control groups, while CD8, macrophage and neutrophil cells were more prominent only in early BHT. The collagenous fibre density were significantly higher only in late BHT, whereas elastic fibre content in late BHT was lower than that in control group. We conclude that the BHT experimental model is pathologically very similar to human usual interstitial pneumonia. This feature is important in the identification of animal models of idiopathic pulmonary fibrosis that can accurately reflect the pathogenesis and progression of the human disease.

Keywords

BHT experimental model, collagen/elastic system, endothelial activity, idiopathic pulmonary fibrosis, microvascular density, type II pneumocytes, usual interstitial pneumonia

Received for publication:
22 November 2007
Accepted for publication:
15 June 2008

Correspondence:
Dr Edwin Roger Parra or
Prof. Vera Luiza Capelozzi
Departamento de Patologia
Faculdade de Medicina da
Universidade de São Paulo
Av. Dr. Arnaldo 455
sala 1143
CEP 01296-903
São Paulo, SP
Brazil
Tel.: 55 11 3066 7427
Fax: 55 11 5096 0761
E-mail: erparra20003@yahoo.com.br
or vcapelozzi@lim05.fm.usp.br

Idiopathic pulmonary fibrosis (IPF) is a chronic fibrosing lung disease associated with the histological appearance of usual interstitial pneumonia (UIP) in surgical lung biopsy. The histological pattern is characterized by alternating areas of normal parenchyma, alveolar collapse, honeycombing and severe mural organizing fibrosis, defined as sites of active remodelling overlying fibrous airspace walls, thus showing temporal heterogeneity, or overlying normal rigid pulmonary structures (e.g. interlobular septa) in the form of fibroblast foci and granulation tissue (American Thoracic Society/-European Respiratory Society 2002). Idiopathic pulmonary fibrosis has several functional repercussions with limiting symptoms and results in important quality of life deterioration. In addition, the currently available treatments present minimal beneficial effects and cause significant side effects. Thus, the identification of the sequential mechanisms involved in the pathogenesis of IPF could help establish the adequate treatment or definitively block pulmonary remodelling.

Recently, some authors have speculated that the structural remodelling in IPF that culminates in interstitial thickening has an early stage, secondary to epithelial type II pneumocyte (TIIp) apoptosis phenomenon, leading to alveolar collapse (Barbas-Filho *et al.* 2001; Baptista *et al.* 2006) and secondary exudative inflammation and a late stage with the incorporation of organizing intra-alveolar fibrosis (Basset *et al.* 1986), involving a degree of vascularization and endothelial activation (Parra *et al.* 2005). Despite advances in knowledge of the pathogenesis in IPF, the temporal evolution of epithelial, vascular and interstitial components of the pulmonary injury in human disease remains a matter of speculation, mainly in the face of sequential structural pulmonary remodelling. Finally, the identification of an experimental model with IPF that shares the morphologic fidelity with the human disease is rare in the existing medical literature, being the first step to establish a true model of the disease.

This study was undertaken to test the hypothesis that structural remodelling of pulmonary parenchyma may be already altered early in IPF evolution. The structural changes would hypothetically reflect the alteration of the alveolar epithelium, microvasculature and connective fibre complex of the alveolar septa. The model and methods used demonstrate the progression of the disease, and result in remodelling within the lungs that is typical of IPF, providing an accurate way to evaluate the relationship between epithelial and interstitial remodelling (amount of type II pneumocytes, collagen and elastic fibres) at different stages of 3-5-di-*tert*-butyl-4-hydroxytoluene (BHT)-induced pulmonary injury.

Material and methods

The experiments were carried out according to the guidelines of the National Institutes of Health, with Institutional Review Board approval for animal experiments. Male Balb/c mice, weighting on average 20 g, were used in the study. The studies were performed in three groups of mice: (i) animals that received BHT and were killed after 2 weeks (early BHT group, nine mice); (ii) animals that received BHT and were killed after 4 weeks (late BHT group, 11 mice); (iii) animals that received corn oil solution (control group, 10 mice).

Induction of pulmonary injury by BHT

In the early and late BHT groups, 400 mg/kg/day of BHT (Sigma Chemical Company, St Louis, MO, USA) dissolved in corn oil was injected in the animals (1.0 ml/kg/day of the dilution) via the intraperitoneal route. In the control group, 1.0 ml of corn oil was injected in the same way as for the BHT groups. The mice were placed in a ventilated Plexiglas chamber with a mixture of pure humidified oxygen and compressed air to maintain the oxygen concentration at 70%. This concentration was periodically monitored by an oxygen analyzer. Six days later, the animals were moved and kept in room air for the rest of the experiment. Food and water were available at all times.

Morphometric studies of the lungs

The animals were sedated, anaesthetized (intraperitoneal pentobarbital sodium, 20 mg/kg) and exsanguinated via the abdominal aorta. The lungs were rapidly removed, dissected and rinsed free of blood with saline solution. Lungs were inflated *in situ* through the trachea at a pressure of 15 mmH_2O, calculated as mice tidal volume and fixed with 10 ml/kg (0.2 ml) of buffered formalin for 6 h. The lungs were then kept in 70% ethanol for 24 h at ambient temperature. Two areas of the lungs, one peripheral and one central, were selected and embedded in paraffin. Histological sections 5 μm thick were obtained and underwent haematoxylin–eosin, immunohistochemistry and specific staining methods to quantify the collagenous [picrosirius-polarization method (Montes 1996)] and elastic system fibres [Weigert's resorcin-fuchsin method (Lemos *et al.* 1997)]. Immunohistochemistry was performed to characterize type II pneumocytes [antibody surfactant apoprotein-A (SP-A), code sc 13977; Santa Cruz Biotechnology, Inc., Santa Cruz, CA, USA; 1:6000 dilution], inflammatory cells [CD4 (monoclonal rat antibody, Santa Cruz Biotechnology, Inc., 1:400

dilution), CD8 (monoclonal rat antibody, Santa Cruz Biotechnology, Inc., 1:100 dilution), macrophage cells (MAC-2), Clone M3/38 Registered Trademark of Cedarlane Laboratories Limited, Toronto, ON, Canada; 1:25,000 dilution], microvasculature (anti-VIII factor antibody, clone QBEend/10; Novocastra Laboratories Ltd, Newcastle, UK; dilution, 1:400), and endothelial adhesion molecule activity [rabbit polyclonal antibody against vascular cell adhesion molecule-1 (VCAM-1), Santa Cruz Biotechnology, Inc., 1:800 dilution]. In brief, the sections were deparaffinized and rehydrated with Tris-buffered saline (TBS: 0.0005 M tri, 0.15 M NaCl), pH 7.6 for 10 min. Endogenous peroxidase was blocked with 3% hydrogen peroxide for 5 min. Next, they were washed in TBS and incubated with primary antibodies at the appropriate dilutions for 1 h. Biotinylated anti-mouse IgG was used as a secondary antibody (DAKO, Carpinteria, CA, USA) followed by peroxidase-conjugated streptavidin (DAKO, Carpinteria, CA, USA). The peroxidase reaction was developed using 3,3′-diaminobenzidine tetrachloride (0.25 mg dissolved in 1 ml of 0.02% hydrogen peroxide) for 3 min.

Collagenous and elastic system fibres were quantified by optical density at the image analysis system in 10 different, randomly selected alveolar septa, as previously described by our group (Rozin *et al.* 2005). The results were expressed as the percentage of the alveolar septal area fraction occupied by the fibres of the collagenous and elastic systems. Surfactant apoprotein-A (SP-A), inflammatory cells, microvascular density (VIII factor) and endothelial adhesion molecule activity (VCAM-1) in the septa were quantified by the point-counting technique. Briefly, at × 400 magnification, we used an eyepiece with a systematic point-sampling grid consisting of 100 points and 50 lines to count the fraction of lines overlying positively stained structures. We averaged the measurements over 10 microscopic fields to obtain a final result as a percentage of stained structures (Gundersen *et al.* 1988). Interobserver comparisons were performed in 20% of the slides by two observers. The coefficient of variation for the interobserver error regarding cell count was <5%.

Statistical analysis

The one-way ANOVA procedure was used for the analysis of variance of TIIp density, vascular density and endothelium activity cells in alveolar septa of early BHT, late BHT and control groups. Differences among the means were compared by Levene's test for homogeneity of variance and then by Bonferroni multiple comparison *post hoc* test. The analysis of variance of collagenous and elastic system fibres between early and late BHT groups was also carried out by Student's *t*-test. The level of significance was established as 0.05. The data were analysed using the SPSS for Windows program, release 10.0 (SPSS Inc., Chicago, IL, USA).

Results

Figure 1 shows that pulmonary BHT injury resulted in two different histological patterns, according to the temporal evolution of the lesions. In the early BHT group (Figure 1a,c,e,g), lung parenchyma showed an intense and temporally uniform appearance, which included diffuse

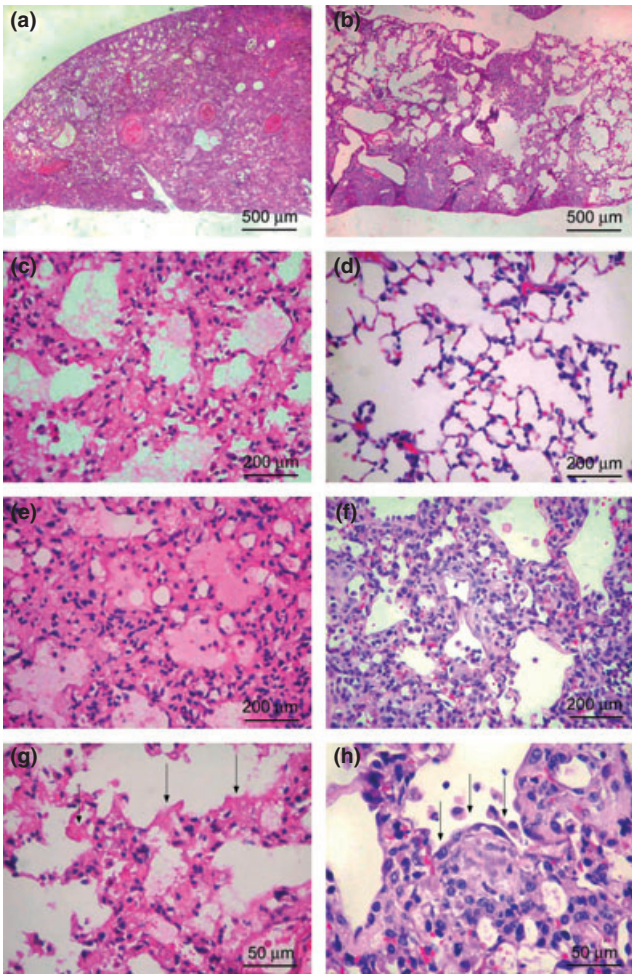

Figure 1 Diffuse alveolar damage lungs showing diffuse involvement and a uniform temporal appearance (a) caused by alveolar collapse and neoseptal formation (c), alveolar oedema (e) and hyaline membranes – arrows (g). Usual interstitial pneumonia lungs showing heterogeneous involvement (b) characterized by normal (d), alveolar collapse (f) and mural organizing fibrosis (fibroblast foci, arrows) (h). h&e: 100× (a,b), 200× (c,d,e,f) and 400× (g,h).

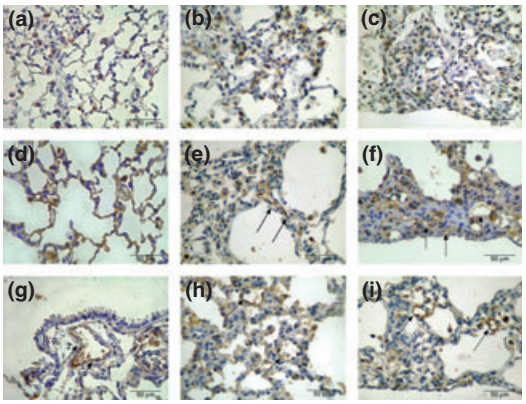

Figure 2 Control group shows the uniform distribution and minimal proportion of SP-A positive cells in alveolar septa (a). In the early BHT (b) group, a homogeneous distribution along the alveolar wall contrasts with a non-homogeneous SP-A profile, poorly distributed along the collapsed and fibroblastic foci areas found in late BHT (c) lungs. Microvasculature immunostaining for factor VIII in the control (d) group shows the uniform distribution coincident with the maintenance of pulmonary architecture. The early BHT (e) group shows diffuse and poor microvasculature density, which is highly active and coincident with the inflammatory alveolar septal thickening. In the late (f) BHT group, a heterogeneous and poor microvasculature density, which is highly active, coincides with the distortion of the pulmonary architecture. VCAM-1 endothelial adhesion molecules in the control (g) is poor, in contrast with significant increase in early (h) and late (i) BHT lungs. Immunostaining for SP-A (a,b,c), factor VIII (d,e,f) and VCAM-1 (g,h,i) was carried out at 400×.

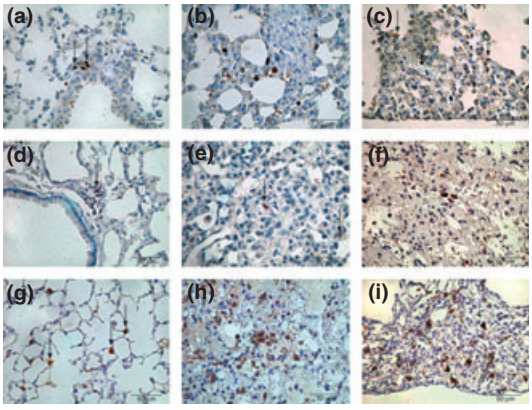

Figure 3 Minimal inflammatory cell involvement by CD4 cells in septal interstitium of control (a) lung contrasts with noticeable CD4 cells in early BHT (b) group, in comparison with late (c) BHT. CD8 immunostaining in septal interstitium shows minimal infiltration in control (d) lungs and a more prominent involvement is present in early (e) compared with late (f) BHT group. The control (g) group shows a small amount of MAC-2 macrophages in alveolar spaces when compared with the more noticeable infiltration in early (h) and late (i) BHT group. Immunostaining for CD4 (a,b,c), CD8 (d,e,f) and MAC-2 (g,h,i) was carried out using 400×.

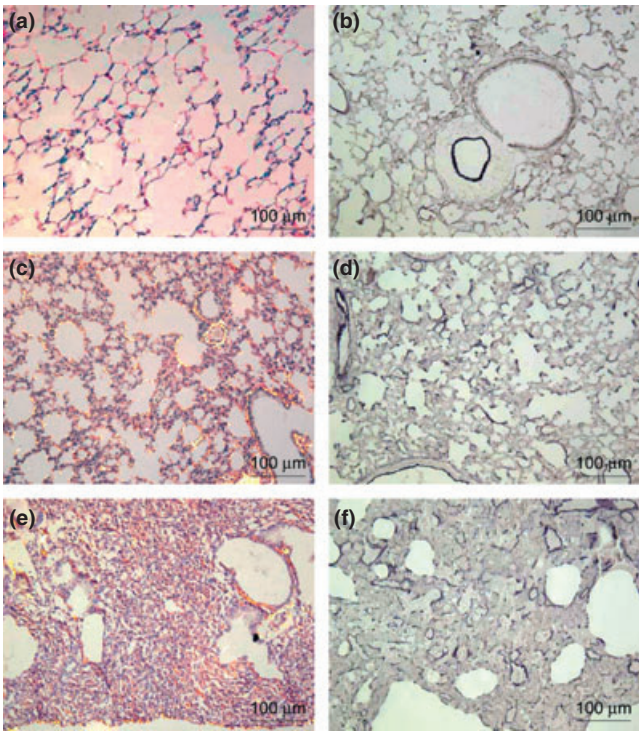

Figure 4 Alveolar septa in control lung showing minimal red-orange birefringence of collagen fibres (a) and minimal elastic fibres (b), whereas alveolar septa in early (c) and late (d) BHT lungs show moderate red-orange birefringence of collagen fibres. In (e) and (f) the elastic system is less prominent in early and late BHT lungs, respectively, when compared with the control group. Picrosirius polarization: a,c,d (200×) and Weigert's Resorcin-Fuchsin: b,e,f (200×).

involvement, alveolar collapse, septal oedema and hyaline membranes in the alveolar spaces, characterizing the diffuse alveolar damage (DAD) pattern. In the late BHT group (Figure 1a,d,f,h), a histological pattern that was similar to UIP was observed, characterized by alternating areas of normal parenchyma, alveolar collapse and initial mural organizing fibrosis, defined by fibroblast foci and granulation tissue in the peripheral acinar areas.

Figure 2 shows SP-A type II pneumocyte immunoprofile in the control (Figure 2a), early (Figure 2b) and late BHT (Figure 2c) lungs. The control group shows the uniform distribution and minimal proportion of TIIp in the alveolar septa. In early BHT group, a homogeneous distribution along the alveolar wall contrasts with a non-homogeneous SP-A profile, poorly distributed along the collapsed and fibroblastic focus areas found in late BHT lungs.

Figure 2 also shows the immunostaining for factor VIII in the microvasculature (Figure 2d–f) and VCAM-1 endothelium adhesion molecules (Figure 2g–i) in the control

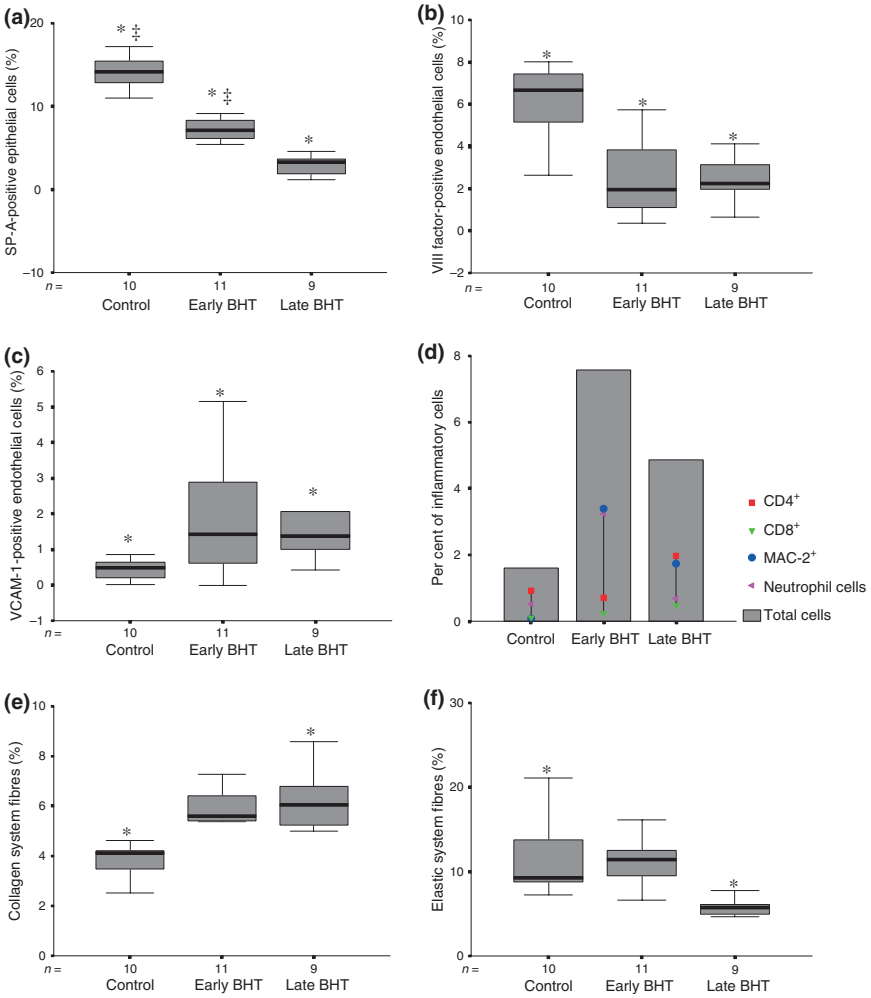

Figure 5 Graphic illustration of type II pneumocytes density (SP-A) (a); microvascular density (VIII factor) (b); vascular adhesion molecule (VCAM-1) (c); inflammatory cells density (d); collagen system fibres density (e); and elastic system fibres density (f) in experimental BHT model and control group. Statistical significance (*) between control groups and early and late BHT group, statistical significance (‡) between early and late BHT group.

(Figure 2d,g respectively), early (Figure 2e,h respectively) and late (Figure 2f,i respectively) BHT lungs. The control group shows the uniform distribution of microvasculature in tissue sections coincident with the maintenance of the pulmonary architecture. In contrast, the early BHT group shows a diffuse and poor microvasculature density that is highly active and coincident with the inflammatory alveolar septal thickening in this group. In the late BHT group, a heterogeneous and poor microvasculature density that is highly active and coincides with the distortion of pulmonary architecture is observed.

Figure 3 shows more cellular involvement by CD4 cells in the septal interstitium of late (Figure 3c) BHT compared with early (Figure 3b) and control groups. As for CD8 in the septal interstitium, a more noticeable involvement is present in early (Figure 3e) compared with late (Figure 3f) and control (Figure 3c) groups. Additionally, the histological analysis in Figure 3h demonstrates a more noticeable infiltration by MAC-2 macrophages in early than in the other groups. Similar conditions are observed regarding the neutrophil cells.

Figure 4 shows the increased content of collagenous and elastic system fibres in the alveolar septa from the lungs in the early (Figure 4c,d respectively) and late (Figure 4e,f respectively) pulmonary injury groups in relation to the control group (Figure 4a,b respectively). Early and late BHT lungs show moderate red-orange birefringence contrasting with minimal red-orange birefringence present in the alveolar septa of the control group. The elastic system is less noticeable in the early and late BHT groups compared with the control group.

Figure 5 shows that the morphological changes in type II pneumocytes, microvasculature and collagenous-elastic systems coincide with the quantification differences among the groups, as well as those concerning the histological patterns (early or late BHT). SP-A-positive type II pneumocytes

(Figure 5a) were significantly decreased in early BHT (7.15 ± 1.30%) and lower in late BHT (3.64 ± 2.61%) when compared with the control group (14.15 ± 2.36%) ($P = 0.03$ and $P < 0.01$ respectively). The vascular density (Figure 5b) is lower in both early (2.47 ± 1.94%) and late (2.49 ± 1.09%) BHT groups when compared with the control group (5.97 ± 2.16%) ($P < 0.001$ and $P = 0.001$ respectively). The endothelial adhesion molecule activity (Figure 5c) observed in early (1.95 ± 1.74%) and late (1.84 ± 1.35%) BHT groups was higher than in the control group (0.43 ± 0.33%) ($P < 0.01$). The amount of CD4 cells in the septal interstitium (Figure 5d) present in the late BHT group (1.96 ± 1.28%) is significantly higher compared with the early BHT (0.71 ± 0.97%) and control (0.92 ± 1.01%) groups ($P = 0.03$). Although CD8 amount in the septal interstitium (0.48 ± 0.61%) was higher than in the early BHT (0.23 ± 0.37%) and control groups (0.09 ± 0.12%), this difference did not achieve statistical significance. However, the amount of MAC-2 macrophages (3.39 ± 1.72%) was significantly higher in the late BHT group than in the early BHT (1.73 ± 0.62%) and control (0.07 ± 0.16%) groups ($P = 0.008$ and $P < 0.001$ respectively). The density of the collagen system fibres showed significantly higher values in the early (5.13 ± 1.19%) and late (6.36 ± 1.37%) BHT groups when compared with the control group (3.78 ± 0.81%) (Figure 5e). Higher amounts of neutrophil cells were observed in the early BHT (3.24 ± 2.14%) when compared with the control (0.51 ± 0.21%) and late BHT (0.68 ± 0.24%) groups ($P < 0.001$ and $P = 0.001$ respectively). Elastic fibre content in the late BHT (5.88 ± 1.02%) was lower than that in the control group (12.01 ± 5.62%) (Figure 5f).

Discussion

This study described an animal model of lung injury and fibrosis that shares some similarities with human IPF/UIP. Idiopathic pulmonary fibrosis/usual interstitial pneumonia is a serious disease with very poor prognosis and most of the patients do not survive for more than 3 years following UIP confirmation. Currently, the lack of knowledge on the pathogenesis of IPF/UIP further increases the urgency and need for research in this area. Therefore, the present study is an important step in the development of a system model to investigate this devastating disease. We demonstrated that a single injection of BHT in mice results in a fibroproliferative condition in the lung with heterogeneous loss of architecture and fibrosis that is characteristic of UIP in humans.

In this study, pulmonary injury was produced by the administration of a single large dose of the antioxidant BHT in mice. BHT, which is the antioxidant butylated hydroxytoluene, accumulates predominantly in the lung and induces alveolar epithelial damage because of its action on type I pneumocytes (TIp) (Hirai *et al.* 1977), which is followed by the proliferation of pulmonary parenchymal cells. Adamson *et al.* (1977), when analysing cell kinetics, reported that 2 weeks after BHT administration, 60% of all dividing cells were TIIp, about 25% were dividing interstitial cells and 10–15% were capillary endothelial cells. After 4 weeks, 50–60% of all dividing cells were interstitial cells and 25–35% were capillary endothelial cells.

The primary model for the study of IPF is the bleomycin-treated rodent; however, neither the acute nor the chronic pulmonary changes resemble UIP (Zia *et al.* 1992), which usually has a peripheral acinar distribution (Borzone *et al.* 2001). Bleomycin administration to mice, rats or hamsters results in pulmonary inflammation and fibrogenesis (Thrall *et al.* 1979) with a more bronchocentric distribution, considering that the induction route of injury in these experiments is usually the intratracheal one (De Rezende *et al.* 2000). Faffe *et al.* (2000) reported a model of acute pulmonary injury that resulted from lipopolysaccharide inhalation, which led to bronchocentric neutrophil infiltration in mouse lung. Our group has published several studies (Rocco *et al.* 2001, 2004; Silveira *et al.* 2004; Xisto *et al.* 2005), reporting acute lung injury produced by the intraperitoneal administration of *N*,*N*′-dimethyl-4,4′-bipyridinium dichloride (Paraquat) in rats. Paraquat is an herbicide that accumulates predominantly in the lung and induces alveolar epithelial damage because of its action on type II pneumocytes, thus reproducing the histological pattern of DAD. None of these models demonstrated the complex lung morphology of the persistent and progressive fibrosis of IPF in humans.

Our study also provides important evidence concerning the temporal evolution of pulmonary injury 2 and 4 weeks following treatment with BHT. The histological patterns of DAD and UIP were very similar to human disease and contrasted with the normal parenchyma from controls. At the histological level, the early and late phases were characterized. In the early phase, lung parenchyma alveolar collapse, septal oedema, and hyaline membranes were observed. In the late stage, alternating areas of normal parenchyma, alveolar collapse and initial mural organizing fibrosis were demonstrated. Type II pneumocytes were decreased in the present model, probably by the noxious action of oxygen on TIIp division. The decrease in SP-A-positive type II cells in this model may indicate either a decrease in the number of type II cells or the expression of SP-A, as we believe that cell proliferation observed in human UIP is represented by Clara cells. Several authors have speculated about the injury mechanism induced by BHT and oxygen cytotoxic action.

According to Adamson *et al.* (1974), the important TIp injury by BHT probably perpetuates the alveolar wall denudation, considering that the TIIp division and TIp differentiation does not reline the alveolar wall. Pulmonary repair, as measured by DNA synthesis, can be inhibited by 16–24-h exposures to 60–100% oxygen on days 2, 3 and 4 after BHT, but not later. Wischi and Côté (1977) postulate that proliferating TIIp are susceptible to the oxygen cytotoxic action, whereas dividing interstitial cells are not. For Haschek and Witschi (1979), the interference with re-epithelialization by the selective killing of epithelial cells would allow excessive proliferation of interstitial cells, leading to the development of fibrosis. Taylor *et al.* (1977) followed by Borok *et al.* (1991) reported that this situation also determines prostaglandin E_2 (PGE_2) decrease and consequently increased fibroblastic proliferation. In summary, decrease in TIIp leads to alveolar collapse and fibrosis. The epithelial cell injury was represented by TIIp decrease and resulted in an extensive denudation of the alveolar-capillary barrier, followed by collagen deposition and elastosis, found mainly in the late stage of BHT. BHT treatment also reduced the number of factor VIII-positive vascular endothelial cells similar to what was reported by Gracey *et al.* (1968)and Renzoni *et al.* (2003) followed by Parra *et al.* (2005) in human UIP, where the neovascularization of injured and fibrotic areas is severely decreased. It is noteworthy that the capillary network diminished from the control to the early and late phase, whereas the opposite occurred in incorporating fibrosis. In fact, establishing a vascular supply is a necessity for any newly formed viable tissue (e.g. proliferative phase endometrium, neoplastic tissues, etc.) and its absence is the equivalent to atrophy. The possibility that early inflammation is important in UIP requires an earlier time point in our study. Increased VCAM following BHT treatment would support inflammatory cell recruitment. In addition, a significant cell involvement by CD4, CD8, macrophage and neutrophil cells is present in the BHT injured lung and allow us to postulate that they may play a role in disease pathogenesis, as previously demonstrated in a previous study by Parra *et al.* (2007). Although it has been suggested in the literature that inflammatory cells and inflammation are a response and not a cause of UIP (Noble & Roberts 2004), the evidence shown in the present study is not convincing. Both collagen and elastic components were increased in the present model, demonstrating a process of fibroelastosis that started early in the injury evolution. The increase in collagen deposition and the decrease/disorganization of elastic elements is consistent with human UIP. In addition, the heterogeneous nature of the injuries and the fibroblast foci give further support to the adequateness of the BHT model.

Our model has limitations. One of them concerns the sample sizes, which were small, although they were enough to achieve statistical significance for the measurements. Additionally, the level of fibrosis observed in the mouse lung 4 weeks following treatment with BHT is minimal, compared with that observed in IPF/UIP in humans. To test the fibrosis progress in this model, we have continued with the experiment with larger sample sizes and a longer 'recovery time', in order to answer this question. Another limitation of this model of IPF is the difficulty to contrast it sufficiently with previously reported models. Unfortunately, the animal models that have been used to study IPF did not appropriately mimic the morphologic changes of IPF. As stated in the National Heart, Lung, and Blood Institute workshop summary, persistent progressive fibrosis with evidence of temporal heterogeneity is a hallmark of IPF; these features are lacking in the contemporary models of lung fibrosis.

We conclude that the BHT experimental model is pathologically very similar to human UIP. The pulmonary histopathology shares most of the features of the human disease. These features include multifocal distribution within the lung, with subpleural orientation, fibroblast focus formation, and fibrosis with collagen fibre accumulation and elastic fibre destruction. The TIIp, the vascular decrease and endothelial cell activation in this model imply in an abnormal alveolar repair of the lung. These features are important in the identification of animal models of IPF that can accurately demonstrate the pathogenesis and progression of the human disease.

Acknowledgements

We are grateful to Biologist Sandra de Morais Fernezlian from the Laboratory of Immunohistochemistry and Dr Welluma Teresa de Souza, D.V.M., for technical assistance. This study was supported by the following Brazilian agencies: the National Council for Scientific and Technological Development (CNPq); Foundation for the Support of Research of the State of São Paulo (FAPESP); and the Laboratories for Medical Research (LIM-05), Hospital das Clinicas, University of São Paulo Medical School.

References

Adamson I.Y., Young L., Bowden D.H. (1974) The type II cell a progenitor of alveolar epithelial regeneration. A cytodynamic study in mice after exposure to oxygen. *Lab. Invest.* **30**, 35–42.

Adamson I.Y.R., Bowden D.H., Côté M.G., Witschi H. (1977) Lung injury produced by butylated hydroxytoluene: cytodynamic and biochemical studies in mice. *Lab. Invest.* **36**, 26–32.

American Thoracic Society/European Respiratory Society (2002) International Multidisciplinary Consensus Classification of the Idiopathic Pulmonary Pneumonia. *Am. J. Respir. Crit. Care Med.* **165**, 277–304.

Baptista A.L., Parra E.R., Filho J.V., Kairalla R.A., de Carvalho C.R., Capelozzi V.L. (2006) Structural features of epithelial remodeling in usual interstitial pneumonia histologic pattern. *Lung* **184**, 239–44l.

Barbas-Filho J.V., Ferreira M.A., Sesso A., Kairalla R.A., Carvalho C.R., Capelozzi V.L. (2001) Evidence of type II pneumocyte apoptosis in the pathogenesis of idiopathic pulmonary fibrosis (IPF)/usual interstitial pneumonia (UIP). *J. Clin. Pathol.* **54**, 132–138.

Basset F., Ferrans V.J., Soler P., Takemura T., Fukuda Y., Crystal R.G. (1986) Intraluminal fibrosis in interstitial lung disorders. *Am. J. Pathol.* **122**, 443–461.

Borok Z., Gillissen A., Buhl R. *et al.* (1991) Augmentation of functional prostaglandin E levels on the respiratory epithelial surface by aerosol administration of prostaglandin E. *Am. Rev. Respir. Dis.* **144**, 1080–1084.

Borzone G., Moreno R., Urrea R., Meneses M., Oyarzún M., Lisboa C. (2001) Bleomycin-induced chronic lung damage does not resemble human idiopathic pulmonary fibrosis. *Am. J. Respir. Crit. Care Med.* **163**, 1648–1653.

Faffe D.S., Seidl V.R., Chagas P.S. *et al.* (2000) Respiratory effects of lipopolysaccharide-induced inflammatory lung injury in mice. *Eur. Respir. J.* **15**, 85–91.

Gracey D.R., Diertie M.B., Brown A.L. Jr (1968) Alveolar-capillary membrane in idiopathic interstitial pulmonary fibrosis electron microscopic study of 14 cases. *Am. Rev. Respir. Dis.* **98**, 16–21.

Gundersen H.J.G., Bendtsen T.F., Korbo L. *et al.* (1988) Some new, simple and efficient stereological methods and their use in pathological research and diagnosis. *APMIS* **96**, 379–394.

Haschek W.M. & Witschi H.P. (1979) Pulmonary fibrosis – a possible mechanism. *Toxicol. Appl. Pharmacol.* **51**, 475–487.

Hirai K.I., Witschi H.P., Cote M.G. (1977) Electron microscopy of butylated hydroxytoluene-induced lung damage in mice. *Exp. Mol. Pathol.* **27**, 295–308.

Lemos M., Pozo R.M., Montes G.S., Saldiva P.H.N. (1997) Organization of collagen and elastic fibers studied in stretch preparations of whole mounts of human visceral pleura. *Ann. Anat.* **79**, 447–452.

Montes G.S. (1996) Structural biology of the fibers of the collagenous and elastic systems. *Cell Biol. Intermed.* **20**, 15–27.

Noble P.W. & Roberts J.H. (2004) Idiopathic pulmonary fibrosis: new insights into pathogenesis. *Clin. Chest Med.* **25**, 749–758.

Parra E.R., da Costa L.R.S., Ab'Saber A.M. *et al.* (2005) Non-homogeneous density of CD34 and VCAM-1 alveolar capillaries in major types of idiopathic interstitial pneumonia. *Lung* **183**, 363–373.

Parra E.R., Kairalla R.A., Ribeiro de Carvalho C.R., Eher E., Capelozzi V.L. (2007) Inflammatory cell phenotyping of the pulmonary interstitium in idiopathic interstitial pneumonia. *Respiration* **74**, 159–169.

Renzoni E.A., Walsh D.A., Salmon M. *et al.* (2003) Interstitial vascularity in fibrosing alveolitis. *Am. J. Respir. Crit. Care Med.* **167**, 438–443.

de Rezende M.C., Martinez J.A., Capelozzi V.L., Simões M.J., Beppu O.S. (2000) Protective effect of aminoguanidine in a murine model of pulmonary fibrosis induced by bleomycin. *Fundam. Clin. Pharmacol.* **14**, 561–567.

Rocco P.R.M., Negri E.M., Kurtz P.M. *et al.* (2001) Lung tissue mechanics and extracellular matrix remodeling in acute lung injury. *Am. J. Respir. Crit. Med.* **164**, 1067–1071.

Rocco P.R., Facchinetti L.D., Ferreira H.C. *et al.* (2004) Time course of respiratory mechanics and pulmonary structural remodelling in acute lung injury. *Respir. Physiol. Neurobiol.* **143**, 49–61.

Rozin G.F., Gomes M.M., Parra E.R., Kairalla R.A., de Carvalho C.R., Capelozzi V.L. (2005) Collagen and elastic system in the remodeling process of major types of idiopathic interstitial pneumonias (IIP). *Histopathology* **46**, 413–421.

Silveira K.S., Boechem N.T., do Nascimento S.M. *et al.* (2004) Pulmonary mechanics and lung histology in acute lung injury induced by *Bothrops jararaca* venom. *Respir. Physiol. Neurobiol.* **139**, 167–177.

Taylor l., Polgar P., McAteer J.A., Douglas W.H. (1977) Prostaglandin production by type II alveolar cells. *Biochem. Biophys. Acta* **572**, 502–508.

Thrall R.S., McCormick J.R., Jack R.M., Ward P.A. (1979) Bleomycin-induced pulmonary fibrosis in the rat: inhibition by indomethacin. *Am. J. Pathol.* **95**, 117–1303.

Wischi H.P., Côté M.G. (1977) Inhibition of butylated hydroxytoluene-induced mouse lung cell division by oxygen: time-effect and dose-effect relationships. *Chem. Biol. Interact.* **19**, 279–289.

Xisto D.G., Farias L.L., Ferreira H.C. *et al.* (2005) Lung parenchyma remodeling in a murine model of chronic allergic inflammation. *Am. J. Respir. Crit. Care Med.* **171**, 829–837.

Zia S., Hyde D.M., Giri S.N. (1992) Development of a bleomycin hamster model of subchronic lung fibrosis. *Pathology* **24**, 155–163.

